Electron-multiplying charge-coupled detector-based bioluminescence recording of single-cell Ca²⁺

Kelly L. Rogers
Plate-forme d'Imagerie Dynamique
Imagopole,
Institut Pasteur
Paris, France
E-mail: krogers@pasteur.fr

Jean-Rene Martin
Bases Neurales des Comportements chez la Drosophile
Laboratoire de Neurobiologie Cellulaire et Moléculaire
Centre National de la Recherche Scientifique
Unité UPR-9040
Gif-sur-Yvette, France

Olivier Renaud
Plate-forme d'Imagerie Dynamique
Imagopole,
Institut Pasteur
Paris, France

Eric Karplus
Science Wares Incorporated
Falmouth, Massachusetts 02540

Marie-Anne Nicola
Marie Nguyen
Plate-forme d'Imagerie Dynamique
Imagopole,
Institut Pasteur
Paris, France

Sandrine Picaud
Unité d'Embryologie Moléculaire
Centre National de la Recherche Scientifique
URA 2578,
Institut Pasteur
Paris, France

Spencer L. Shorte
Plate-forme d'Imagerie Dynamique
Imagopole,
Institut Pasteur
Paris, France

Philippe Brûlet
Unité d'Embryologie Moléculaire
Centre National de la Recherche Scientifique
URA 2578,
Institut Pasteur
Paris, France

Abstract. The construction and application of genetically encoded intracellular calcium concentration ($[Ca^{2+}]_i$) indicators has a checkered history. Excitement raised over the creation of new probes is often followed by disappointment when it is found that the initial demonstrations of $[Ca^{2+}]_i$ sensing capability cannot be leveraged into real scientific advances. Recombinant apo-aequorin cloned from *Aequorea victoria* was the first Ca^{2+} sensitive protein genetically targeted to subcellular compartments. In the jellyfish, bioluminescence resonance energy transfer (BRET) between Ca^{2+} bound aequorin and green fluorescent protein (GFP) emits green light. Similarly, Ca^{2+} sensitive bioluminescent reporters undergoing BRET have been constructed between aequorin and GFP, and more recently with other fluorescent protein variants. These hybrid proteins display red-shifted spectrums and have higher light intensities and stability compared to aequorin alone. We report BRET measurement of single-cell $[Ca^{2+}]_i$ based on the use of electron-multiplying charge-coupled-detector (EMCCD) imaging camera technology, mounted on either a bioluminescence or conventional microscope. Our results show for the first time how these new technologies make facile long-term monitoring of $[Ca^{2+}]_i$ at the single-cell level, obviating the need for expensive, fragile, and sophisticated equipment based on image-photon-detectors (IPD) that were until now the only technical recourse to dynamic BRET experiments of this type. © *2008 Society of Photo-Optical Instrumentation Engineers.* [DOI: 10.1117/1.2937236]

1 Introduction

$[Ca^{2+}]_i$ fluctuations are most commonly considered and certainly most easily described according to their analog waveform characteristics, *i.e.*, amplitude and frequency. This also reflects the fact that Ca^{2+} signaling functions are widely believed to depend on distinct waveform encoded signal patterns controlling, for example, up- and down-regulation of selected gene expression.[1,2] Such hypotheses have proved technically challenging to test, in as much as functional (nonpathological) Ca^{2+} signal fluctuations can display durations between milliseconds to minutes, and resonate in oscillatory states where frequency can vary widely.[3,4] Furthermore, distinct ordered patterns of functional Ca^{2+} signaling activity can occur at unpredictable intervals (minutes, to hours, to days) during otherwise long periods of quiescence.[5] For all these reasons,

Address all correspondence to Kelly Rogers, PhD, Plate-forme d'Imagerie Dynamique, Institut Pasteur, 25 Rue du Docteur Roux, 75724 Paris Cedex 15, France; Tel: +33 1 4061 3177; Fax: +33 1 4568 8949; E-mail: krogers@pasteur.fr

the major criterion for a method to monitor Ca^{2+} signals is that it should allow one to follow a broad range of dynamic phenotypes continuously, noninvasively, and during unlimited periods of time. Currently, the most widely used methods for monitoring $[Ca^{2+}]_i$ depend on fluorescence imaging methods that do not fulfill these requirements.

The discovery of photoproteins in organisms like *Aequorea sp.* and *Photinus pyralis* revolutionized the field of optical imaging. In the *Aequorea* jellyfish, two photoproteins were isolated and later cloned, including green fluorescent protein (GFP) and the Ca^{2+} sensitive bioluminescent protein, aequorin.[6–9] When isolated, Ca^{2+} binding to aequorin causes an intramolecular oxidation of its bound chromophore substrate, coelenterazine, resulting in the emission of blue light (λ 470 nm). In contrast, the isolated GFP emits green light (λ 509 nm) on excitation λ 475 nm, making it a useful gene expression reporter. In the jellyfish, the two proteins are located in close enough proximity so that the energy transition from the Ca^{2+}-bound aequorin oxidation of coelenterazine is transferred nonradiatively to GFP, resulting in the emission of green light, a process known as bioluminescence resonance energy transfer (BRET).[10]

As an optical Ca^{2+} reporter probe with a low Ca^{2+} binding affinity, aequorin provided one of the first opportunities to address questions concerning signal transduction by high $[Ca^{2+}]_i$ domains.[11] Since apoaequorin was cloned, it has also been used extensively to selectively measure $[Ca^{2+}]$ in subcellular compartments like the mitochondrial matrix and the endoplasmic reticulum.[12,13] However, detection of the very weak luminescence of aequorin required high-sensitivity photon detection devices, limiting the possible applications for living intact cell work, and the method was largely abandoned (where it concerned single-cell measurements) in favor of Ca^{2+} sensitive fluorescent dyes,[14] and more recently, genetically encoded calcium sensitive fluorescent proteins.[15–18] Here we demonstrate how very recent cutting-edge advances in photon detector cameras, optical microscopy, and molecular probe technologies promise to greatly simplify and improve the use of semi quantitative bioluminescence imaging, and are promising a renaissance for the use of aequorin to measure intracellular calcium concentrations ($[Ca^{2+}]_i$).

2 Materials and Methods

2.1 Cell Culture and Transfection

Neuro2A and HEK-293 cells were grown in Dulbecco's Modified Eagle's Medium (DMEM) supplemented with 10% Fetal Calf Serum (FCS) (Invitrogen, Life Technologies). Cultures were incubated at 37°C in a humidified atmosphere of 5% CO_2. Cells were transfected using FuGENE transfection reagent (FuGENE®6, Roche, France) when below 50% confluency, and left in culture for 24 to 48 h before the beginning of the experiments. Cells were then incubated with either native or *h* coelenterazine (5 μM, see http://www.interchim.com/) for 1 to 2 h prior to experiments. For experiments on neuro2A cells, cultures were serum-starved 24 h prior to the beginning of experiments to induce apoptosis.[19] In other experiments, HEK-293 cells were stimulated with different concentrations of ATP (0.03 to 3 mM) and were then recorded with an electron-multiplying charge-

coupled detector (EMCCD) on the Luminoview system or on a conventional microscope (details discussed later). ATP disodium salt (see http://www.sigmaaldrich.com/) was dissolved in deionized H_2O to a final concentration of 100 mM and diluted further with phosphate buffered saline (PBS) prior to cell application. For stimulation of cells, 100 μl of ATP solution was added by pipette to the MatTek dish (35 mm; see http://www.glass-bottom-dishes.com/) containing monolayers of HEK-293 cells and 900 μl of medium. The dark box was then closed and acquisition started immediately.

2.2 Transgenic Drosophila Melanogaster

The generation of transgenic *D. melanogaster* expressing GFP-apoaequorin was previously described.[19] Briefly, pG5A[20] was inserted into the pUAST vector and transformants were then crossed with the *P[elav-GAL4]C155* fly line from the Bloomington Stock Center (Bloomington, IN). Elav is expressed exclusively in neurons from midembryogenesis up to and including adulthood.

2.3 Bioluminescence Imaging

Where indicated, the Ca^{2+}-dependent luminescence of GFP-aequorin was detected using an imaging photon detector (IPD 3, Photek Limited, East Sussex, United Kingdom) on the baseport of a widefield inverted microscope (Axiovert 200M, Zeiss, Germany).[21] The IPD is a position-sensing high gain photomultiplier tube using a cascaded stack of four multichannel plates [for a more detailed description, see http://www.photek.co.uk/phoprodf3.htm and, Ref. 22]. It consisted a bialkali photocathode and fiber optic input window. According to the manufacturer's data, the sensitivity of the detector was highest in the blue to green wavelength range with quantum efficiencies ranging from 12.7% at 400 nm to 5.2% at 532 nm, and a dark noise of 4 cps/cm^2 with a spatial resolution of 62 μm at the photocathode surface. A 40× oil objective lens with a numerical aperture (NA) of 1.3 was used in Neuro 2A studies, and a 20× objective lens with a NA of 0.6 was used for studies on the fly brain. The detector, microscope, antivibration table, and fiber optics were housed inside a light-tight dark box (see, http://www.sciencewares.com/). Both the epifluorescence and halogen lamps were mounted outside the black box and connected via light guides to the microscope. The software enables automation of acquisition by the IPD or the CCD when the blackbox is closed (IPD for Windows 95, see http://www.sciencewares.com/). Ca^{2+}-induced bioluminescent signals were monitored continuously over long periods (hours) using the IPD (see Refs. 19 and 21 for more details). For correlation to cell morphology, luminescence imaging was interrupted briefly so that brightfield or epifluorescence images could be periodically taken with a CCD connected to the microscope C-port. In studies on neuro2A cells undergoing apoptosis, brightfield images were taken once every hour.

Single-cell Ca^{2+}-induced luminescence of GFP-aequorin was also monitored with an electron multiplier CCD camera (Hamamatsu, Back-Thinned Frame Transfer, EM-CCD, C9100-13, 8.2×8.2-mm image area, 512×512 pixels, cooled to −65°C) mounted on the baseport of a microscope optimized to detect luminescence (LV200, Luminoview
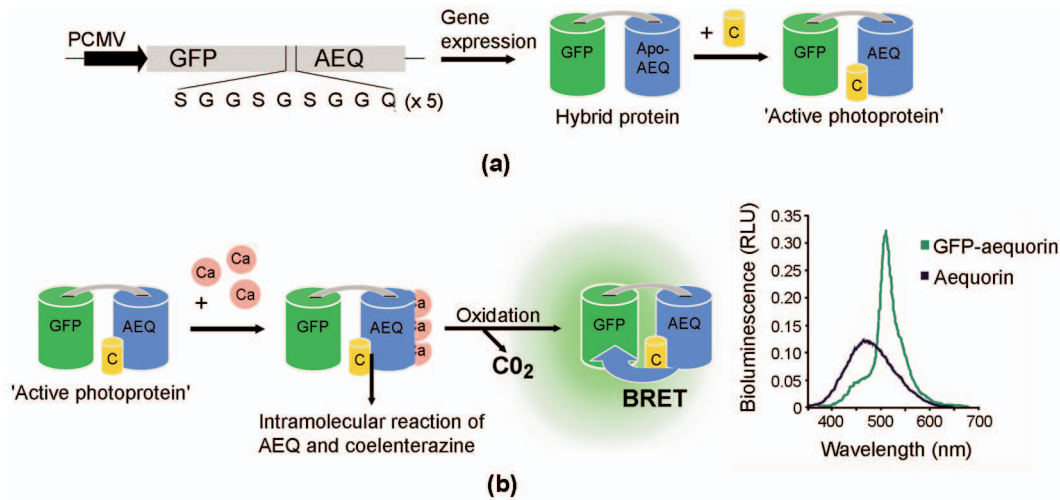
Fig. 1 Schematic diagram of the genetically encoded hybrid protein, GFP-aequorin, and the measurement of [Ca^{2+}] by BRET. (a) Schematic map of the GFP-apoaequorin construction. The hybrid protein consists a GFP fusion via a flexible linker to apo-aequorin. After expression in cells, the apo-aequorin must be reconstituted with the chromophore substrate, coelenterazine (C), to produce the active form of the photoprotein aequorin (noncovalent complex of apo-aequorin and coelenterazine). The hybrid protein is a dual reporter where the localization of the protein in cells can be monitored by the fluorescence of GFP (λ 509 nm). (b) The binding of Ca^{2+} ions to aequorin causes oxidation of the bound coelenterazine, which decomposes into coelenteramide and CO$_2$. Energy is then transferred nonradiatively to GFP and light is emitted having a peak emission in the green (λ 509 nm) (see the resulting bioluminescence spectrum in green). Shown also is the spectrum for aequorin (blue trace), which has a peak emission in the blue (470 nm).
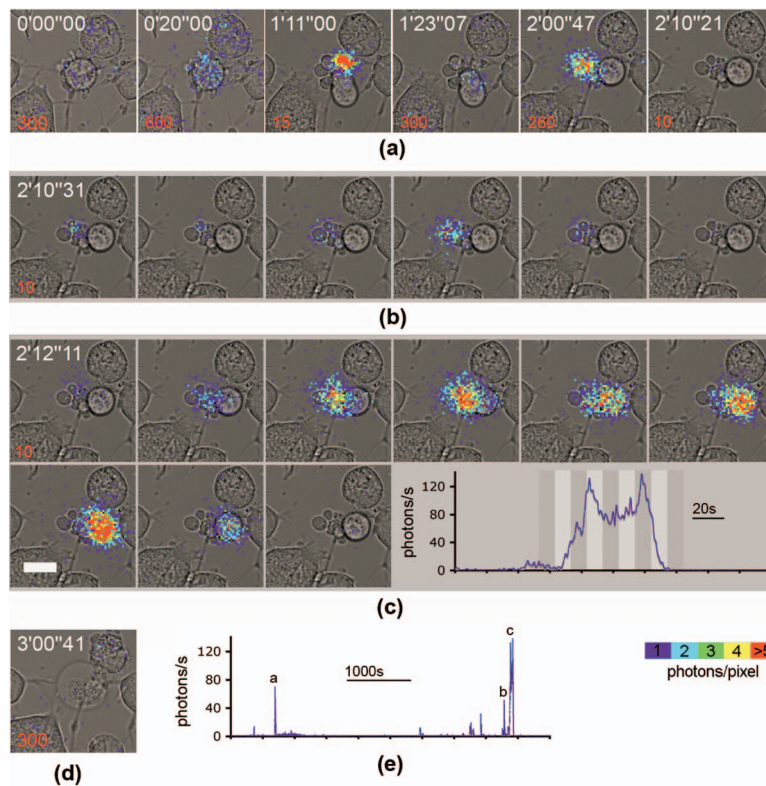

Fig. 2 Single-cell bioluminescence studies of Ca^{2+} signaling using an image photon detector (IPD). Neuro-2A cells transfected with GFP-apoaequorin were serum-starved for 48 h and then recorded continuously using an IPD for up to 10 h. Frames shown are pseudocolor-coded bioluminescence images superimposed to corresponding brightfield images (taken periodically, once every hour). (a) Bioluminescent images were integrated for different durations according to their light intensities (the time is indicated in red in the bottom left-hand corner of each frame) and at different time points during the acquisition (indicated in white). The times indicated at the top of each frame are relative to the first frame, which is designated 0'00"00. (b) and (c) Consecutive 10-s frames (enclosed in gray boxes) from two different time points. (c) Corresponding plot of the light intensity versus time for the frames in (c) (indicated on the plot as dark and light gray vertical lines). (d) Last frame showing a 300-s light integration. (e) Overall plot of the light intensity (photons/s) and corresponding to the images shown. A 40× oil objective (1.3 NA) was used. Resolution is 512×512. Scale bar=10 μm.

Olympus Corporation, Japan). The luminescence imaging microscope is optimized for greater light collection by using high NA objectives and through improvements to the transmission efficiency of each optical element. In addition, the brightness of the image is further enhanced by a $0.2\times$ magnification lens behind the objective, which enables a larger field of view (FOV) to be projected onto a smaller chip area (8.2×8.2 mm). In experiments here, we used a $60\times$ oil objective (1.35 NA), which gave a final image magnification of $12\times$ and FOV of approximately 682.5×682.5 μm.

Single-cell imaging was also undertaken with an EMCCD (iXon DV887 back-illuminated, 512×512 array of 16×16 μm pixels cooled to -70°C, Andor Technology, Belfast, UK) mounted on the baseport of a conventional microscope (200M, Zeiss, Germany). According to spectral response data for both cameras, the quantum efficiency of each EMCCD ranged from 90% at 500 and 600 nm, to 87% at 700 nm and 70% at 800 nm. In both cases, the imaging chamber and objectives were housed inside a light-tight dark box.

2.4 Electron-Multiplying Charge-Coupled Detector and Image Photon Detector Low-Light Imaging Studies

In studies investigating the performance of the IPD and the EMCCD, both cameras were mounted on a Zeiss Axiovert 200M microscope, and light from light-emitting diodes (LEDs) was detected simultaneously using a 50/50 beamsplitter. Specifically, the IPD (IPD425, bialkali or S20 photocathode, Photek, United Kingdom) was mounted on the sideport with a $0.5\times$ reducing lens (Zeiss to C-mount adapter), and the EMCCD (DV897, Andor Technology, 512×512 array of 16×16 μm pixels) was mounted on the baseport. The DV897 was operated at 3.5 Hz (285.64-ms time resolution) and cooled to -80°C. Light was then projected through a pinhole onto an 1.2-mm area using a 430- or 555-nm LED. A triangle wave voltage in series with a load-limiting resistor was applied to the photodiode, which produced light with a softened peak.

3 Results and Discussion

3.1 Calcium-Dependent Green Fluorescent Protein Aequorin Bioluminescence

Recently it has been demonstrated that aequorin fusion to fluorescent proteins like GFP,[19–21,23–25] enhances and facilitates its utility as an *in-situ* Ca^{2+} ion probe [Fig. 1(a)]. These chimerical proteins undergo a so-called bioluminescent resonance energy transfer (BRET) in a $[Ca^{2+}]$-dependent manner. Thus, while gene expression of the reporter can be monitored via GFP fluorescence, Ca^{2+} signals are measured (in the absence of excitation light) simply by detecting green (>509 nm) light emission because the light excited energy (>460 nm) derived from the reaction of aequorin, Ca^{2+}, and coelenterazine is transferred nonradiatively to the GFP moiety [Fig. 1(b)]. That Ca^{2+} signals can be detected without need for light excitation arguably provides what may be considered one of the most significant advantages of bioluminescence experimental design over fluorescence-based methods: the absence of excitation light-induced phototoxicity. This is illus-

trated in a simple experiment based on the paradigm of *spontaneous* neuronal cell death (Fig. 2).

Using Neuro2A cells we aimed to record $[Ca^{2+}]_i$ fluctuations during spontaneous cell death occurring in culture. Enhanced probability of spontaneous cell death came in the absence of serum, and the presence of millimolar quantities of extracellular calcium. In this case, our prior knowledge of the experimental system allowed us to estimate the approximate time window (several hours) over which cell death might occur, but not the exact moment. Further, while the role of $[Ca^{2+}]_i$ fluctuations is strongly suggested, the exact $[Ca^{2+}]_i$ "signature" remained completely unknown. Using GFP-aequorin, we were able to continuously record $[Ca^{2+}]_i$ in a small field of cells during several hours with only brief interruptions, so that transmission snapshots could be monitored for spontaneous cell-death-associated changes (e.g., membrane blebbing and nuclear chromatin condensation). Cells displaying changes corresponding to spontaneous death were eventually identified easily from transmission light images. In all cases, analysis of related cellular changes was accompanied by short repeat bursts of Ca^{2+} spiking patterns [Figs. 2(a)–2(c)]. Occasional individual spiking bursts of activity comprised prolonged (tens of seconds) plateaus superimposed by low- to high-frequency low-amplitude oscillations [e.g., Fig. 2(c)]. Initially, such bursts occurred occasionally, but eventually became more frequent as cell death progressed further during some 90 min [Fig. 2(e)] until cataclysmic cell death occurred [Figs. 2(d) and 2(e)]. These data indicate that at least for Neuro2A cells cultured under these conditions, spontaneous cell death events occur accompanied by distinct $[Ca^{2+}]_i$ fluctuation patterns. Such a conclusion would be difficult to draw based on measurements using calcium-sensitive fluorescent dyes (e.g., Fura 2)[14] or genetically encoded proteins[16] because continuous excitation illumination itself can lead to phototoxicity and cell death.[26]

3.2 Monitoring $[Ca^{2+}]_i$ by Bioluminescence In Vivo

In addition to frequency and amplitude, the spatial aspect of Ca^{2+} signaling at the level of cell-cell networks is widely believed an important aspect of Ca^{2+} information coding *in vivo*. This again presents a technical challenge, wherein ideally methods for detecting $[Ca^{2+}]_i$ fluctuations should maintain high temporal resolution, over long durations, *and* be capable to detect simultaneously cell-cell network propagation where spatially heterogeneous signals cross many hundreds of microns to millimeters. Along these lines, GFP-aequorin bioluminescence-based methods for measuring calcium are singularly powerful.

Like other genetically encoded probes, GFP-apoaequorin can be targeted to subcellular compartments,[21] or to specific cell types by transgenesis.[19,24] However, the advantage of using GFP-aequorin and bioluminescence is especially apparent considering the latter paradigm (Fig. 3 and Video 1). Ca^{2+}-dependent bioluminescent signals were detected *in vivo* in transgenic flies expressing GFP-aequorin exclusively in neurons of the brain. Prolonged recordings during more than ten hours allowed "spontaneous" Ca^{2+} signals with highly variable kinetic properties to be visualized in different areas of the fly brain [Figs. 3(a) and 3(b)]. These results highlight the capacity of this approach to resolve dynamic processes
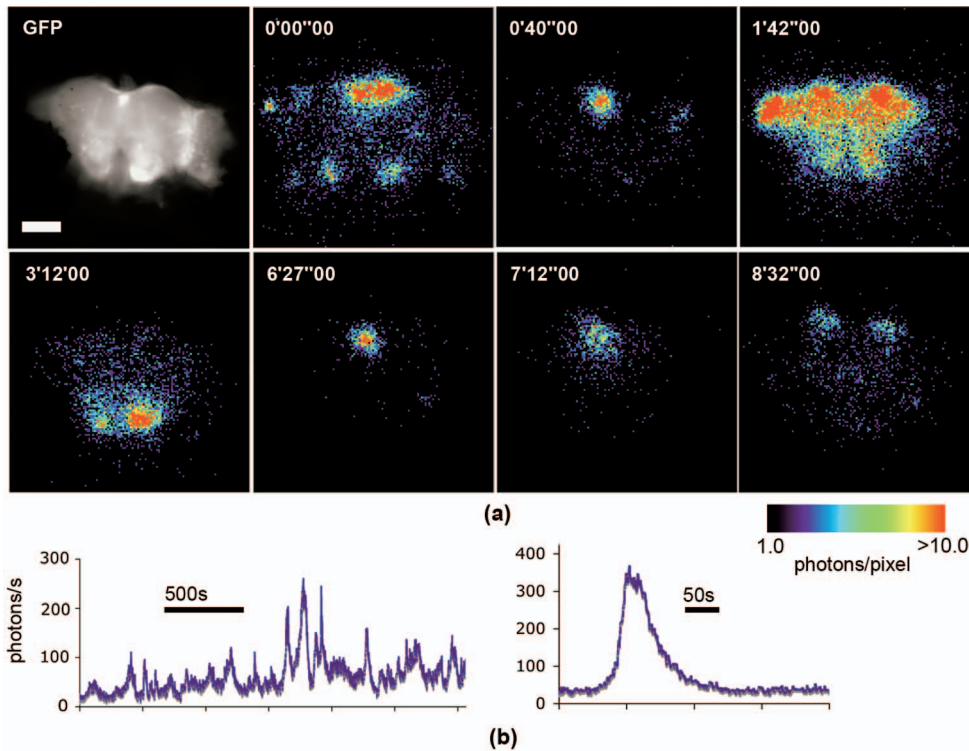
Fig. 3 Long-term recordings of Ca^{2+}-induced bioluminescence in the living fly brain. Ca^{2+}-induced bioluminescent signals were recorded for more than 8 h in *D. melanogaster* expressing GFP-apoaequorin exclusively in neurons (elav-gal4). (a) First frame showing a GFP fluorescence image of the brain after removal of the head capsule. Subsequent frames show pseudocolor-coded bioluminescent images (128×128 pixels), where the total light was integrated over 300 s. Indicated times on each frame are relative to the first frame that is designated 0'00"00. (b) The total flux (photons/s) of the entire recording area is plotted as a function of time. The plots show two examples of shorter data segments derived from the entire light recording. A $20\times$ dry objective lens (0.6 NA) was used. Scale bar=50 μm.

like Ca^{2+} signaling across a wide temporal range and simultaneously across wide areas containing multiple regions of interest. This is particularly useful for exploratory type studies where the characteristics of Ca^{2+} signals are unknown or highly variable, and/or unpredictable.

3.3 Electron-Multiplying Charge-Coupled Detector Detection of Ultralow Light Signals

As illustrated by previous examples with GFP-aequorin, IPD-based photon-counting detector technologies have to date pro-
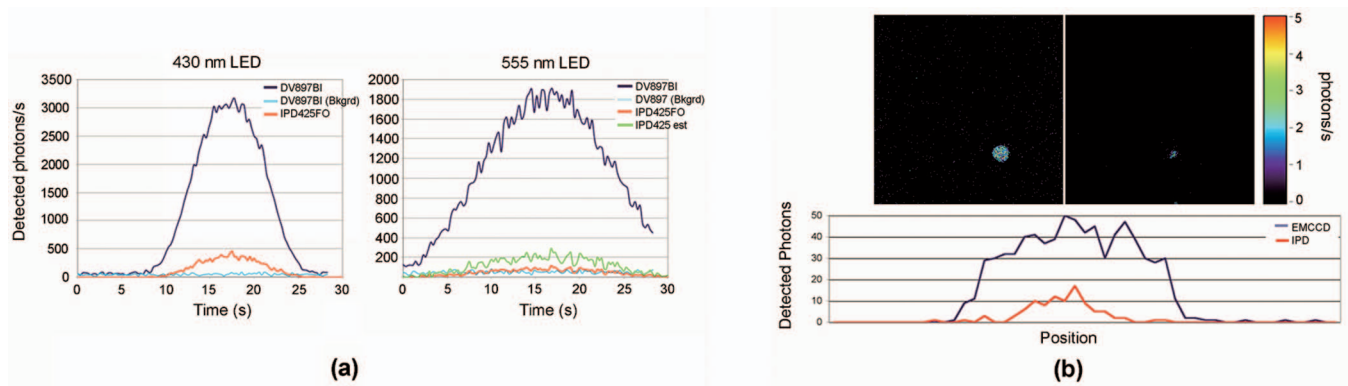

Fig. 4 Ultralow light level detection by the EMCCD and IPD detector. Light from a source LED was then detected through a 50/50 beamsplitter, by an IPD (bialkali or S20 photocathodes) mounted on the sideport and the EMCCD on the baseport of a Zeiss Axiovert 200M microscope (see Methods in Sec. 2 for details). (a) Plot of photons detected from a source LED (430 and 555 nm, in series with a limiting resistor and driven by a triangle wave voltage source) versus time (s). (b) Same experiment as before but comparison of the spatial resolution of the IPD and the EMCCD at 555 nm. Bioluminescent images (1-s panels) show results for the EMCCD (left panel) and the IPD (right panel). Plot of the light intensity versus the position of the detected photons, where both images have the same physical scale.
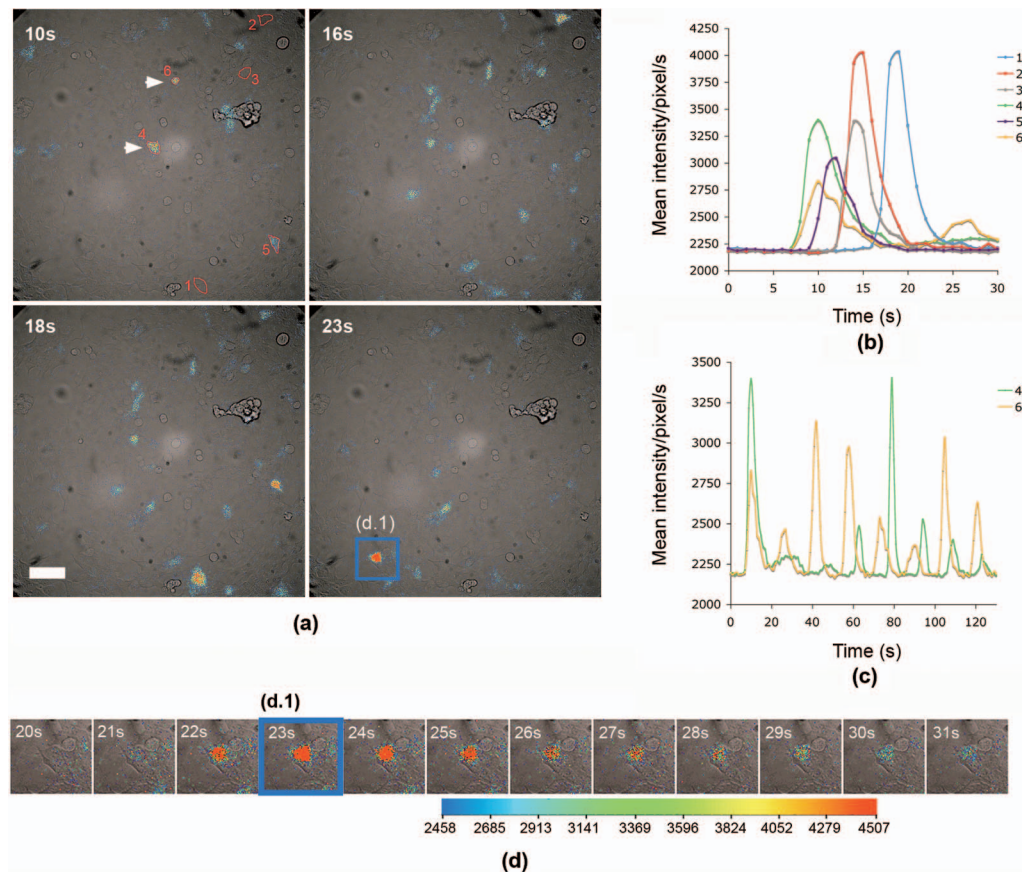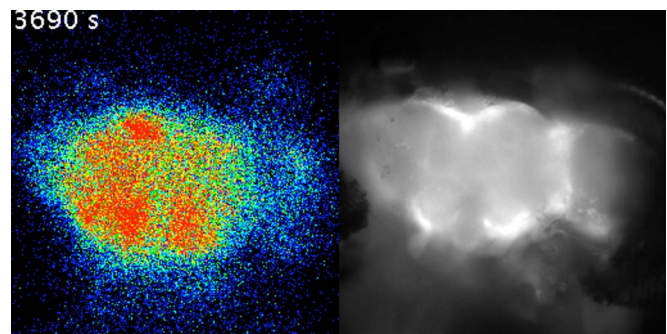
Fig. 5 Detection of ATP-induced Ca^{2+} oscillations in HEK-293 cells with an EMCCD mounted on a microscope optimized for light collection. HEK-293 cells growing in glass bottom chambers (MatTek, 35 mm) were transfected with GFP-apoaequorin (G5A). After incubation with native coelenterazine (5 μM), cells were mounted onto an inverted microscope (LV-200, Olympus). Cells were stimulated by addition of ATP to a final concentration of 30 μM. (a) Frames show pseudocolor-coded bioluminescence images (mean intensity/pixel) superimposed with the brightfield image (taken at the end of acquisition). The bioluminescence of each frame was integrated during 1 s from the times indicated (where 0 s represents the start of acquisition). The scale bar = 50 μm. (b) Analysis of the light intensity (mean intensity/pixel/s) versus time in selected ROIs shown in the first frame of (a). Data in the plot show the first peak in light intensity following application of ATP (30 μM). (c) Extended graph from (b), showing examples of ATP-induced $[Ca^{2+}]_i$ oscillations detected in two cells marked with closed arrowheads in (a) (also ROI 4 and 6). (d) Data zoom of a single cell showing the ATP-induced $[Ca^{2+}]_i$ rise in consecutive frames. (d.1) Corresponds to the last frame in (a). 60× oil objective (1.35 NA). Resolution is 512×512.

vided the means to measure bioluminescence in single cells.[21,27] and intact organs/tissues.[19] However, IPD technology has a number of disadvantages. Notably, IPD detectors are expensive and sophisticated; they are highly vulnerable to irreversible light damage, and quantum efficiencies are low (QE=10%) with respect to genetically encoded fluorescent protein tags in common use, including GFP. These facts have strongly discouraged the routine use of IPD detectors and therefore single-cell bioluminescence in laboratories lacking the technical expertise to host this type of equipment. Fortunately, dependence on IPD detectors as the unique recourse to achieve single-cell bioluminescence detection has very recently been overturned by the development of EMCCD cameras,[28,29] a new generation of highly sensitive detectors measuring ultralow light levels with modest integration times (seconds). Further, in complete contrast to IPDs, EMCCDs are extremely resistant to light damage, and provide robust quantum efficiency in excess of 70% throughout most of the visible spectrum (wavelengths 450 to 800 nm), and as high as 90% from 500 to 650 nm. We simultaneously compared the

Video 1 Video showing part of the long-term recording of Ca^{2+}-induced bioluminescence in the living fly brain, which is represented in Fig. 3. Each bioluminescent frame is pseudocolor coded (0 to 5 photons/pixel) and represents 30 s of accumulated light (10 frames/s). A GFP fluorescence image of the brain is shown in the right-hand frame. Resolution is 256×256 (QuickTime, 17.6 MB). [URL: http://dx.doi.org/10.1117/1.2937236.1].
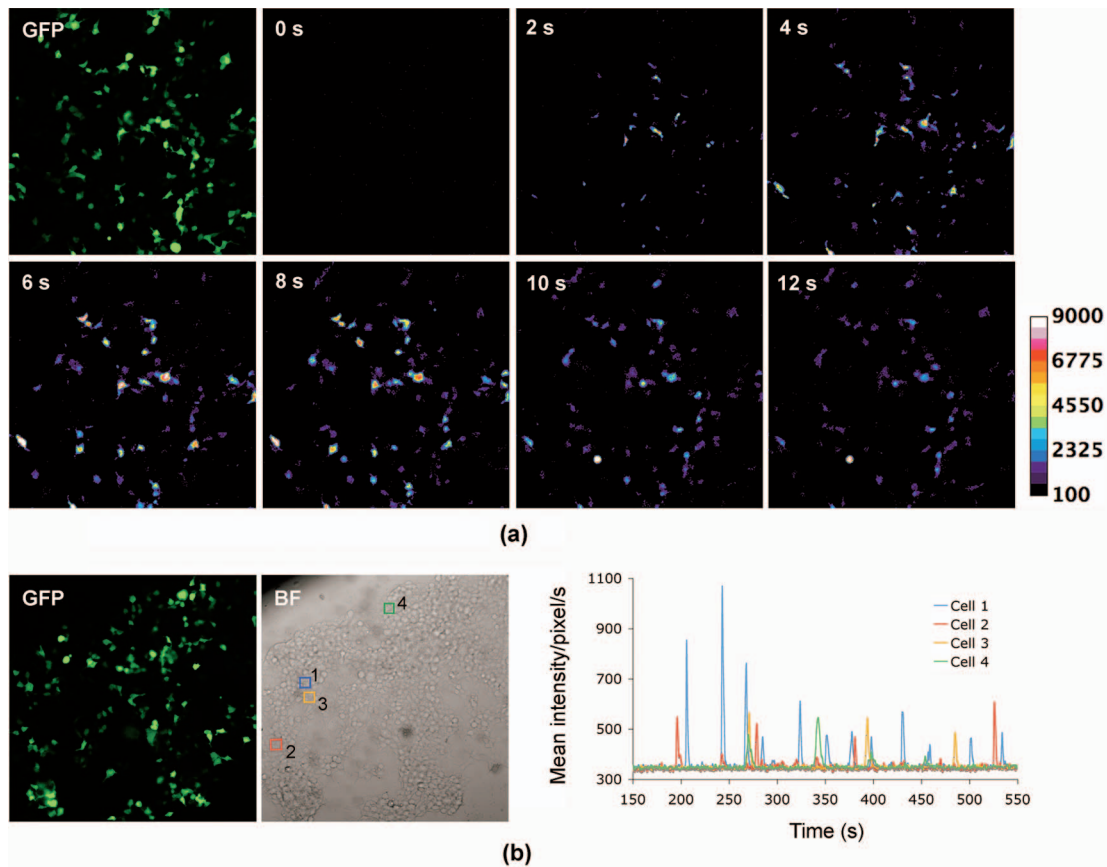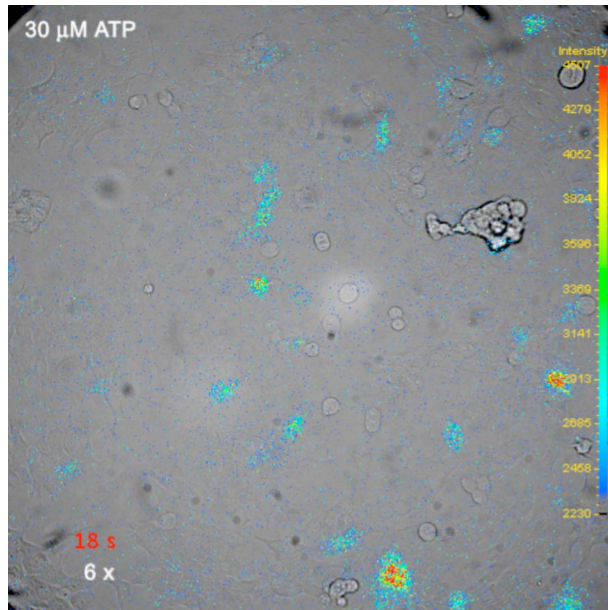
Fig. 6 Detection of ATP-induced Ca^{2+} oscillations in HEK-293 cells with an EMCCD mounted on a conventional microscope. HEK-293 cells growing in glass bottom chambers (MatTek, 35 mm) were transfected with GFP-apoaequorin (G5A). After incubation with coelenterazine h (5 μM), cells were mounted onto an inverted microscope (200M, Zeiss, Germany) and the acquisition was started immediately after addition of ATP. (a) Stimulation with 3-mM ATP. The first frame shows the GFP fluorescence image (512×512) and is followed by consecutive bioluminescence images (0 s represents the start of acquisition). Bioluminescent frames were each integrated for 2 s and are pseudocolor coded (mean light intensity/pixel). (b) Stimulation with 30-μM ATP. GFP fluorescence (left) and brightfield (right) images of HEK-293 cells transfected with G5A. Graph shows a plot of the light intensity (mean intensity/pixel/s) versus time in four cells (marked on the brightfield image). Each frame was integrated for 1 s. A $10\times$ dry objective (0.5 NA) and resolution of 256×256, binning 2, was used in both (a) and (b).

performance of each camera (IPD on the sideport versus EM-CCD on the baseport) by detecting the light output from a source LED (in series with a limiting resistor and driven by a triangle wave voltage source) through a 50/50 beamsplitter (see methods for details). At two wavelengths (430 versus 555 nm), the IPD (bialkali photocathode) detected less photons overall, but the ratio of the detected signal over the noise of the IPD was far superior to that obtained on the EMCCD [Fig. 4(a)]. This means that the IPD should provide a much better temporal resolution than the EMCCD. On the other hand, the QE of the EMCCD is significantly higher than the IPD, which means that overall the EMCCD detects a lot more photons and will give better counting statistics, providing that the dark noise inside an ROI is kept below 10% of the statistical noise limit [Fig. 4(a)]. In addition, our results showed that the spatial resolution of the EMCCD was at least twice as good as that obtained on the IPD [Fig. 4(b)].

3.4 Facile Long-Term Continuous Measurement of Single-Cell Ca^{2+}-Dependent Bioluminescence

The temporal resolution of the EMCCD can be improved by at least two means. First, by increasing the total amount of
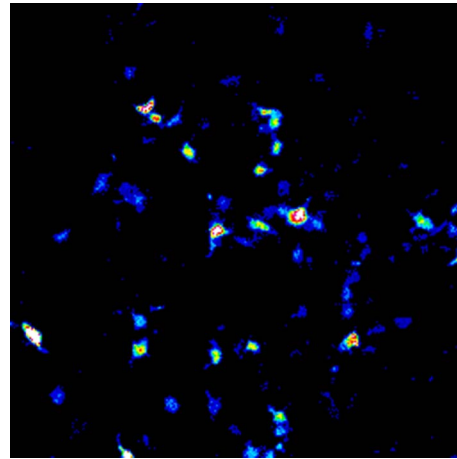
light that can be collected, and second, by enhancing the light emission of the bioluminescence reaction. In the first case, using optics with a high numerical aperture and transmission efficiency can optimize light collection.[30] Very recently, one microscope manufacturer released a dedicated bioluminescence imaging microscope (Luminoview, LV-200, Olympus Corporation, Japan) designed to yield significantly greater amounts of light collection compared to a conventional light (epifluorescence) microscope. The improvement in photon collection performance comes from a proprietary adaptation of the internal light relay optics, which we predicted in combination with an EMCCD device should provide for overall bioluminescence imaging performance at least as well as conventional IPD methods, and with more practical (robust) characteristics. Along these lines, we tested the combination of a highly sensitive EMCCD (Hamamatsu C9100-13), see Materials and Methods in Sec. 2 porting a so-called back-thinned CCD chip that provides the very highest photon sensitivity, combined with very low noise. As a target, we measured ATP stimulated purinergic receptor-driven Ca^{2+} fluctuations in HEK-293 cells (transfected to express GFP-apoaequorin) (Fig. 5 and Video 2). The addition of ATP to culture medium

Video 3 Video showing $[Ca^{2+}]_i$ rises in HEK-293 cells in response to the application of ATP (3 mM). Video corresponds to data in Fig. 6(a). Bioluminescent frames are pseudocolor coded and were integrated for 2 s each (7 frames/s). Resolution is 256×256, binning 2 (Quick-Time, 0.632 MB). [URL: http://dx.doi.org/10.1117/1.2937236.3].

Video 2 Video showing $[Ca^{2+}]_i$ rises in HEK-293 cells in response to the application of ATP (30 μM). Video corresponds to data in Fig. 5. Bioluminescent frames are superimposed on the brightfield image taken at the end of the experiment. Each frame is pseudocolor coded (scale is shown) and was integrated for 1 s (6 frames/s). Resolution is 512×512. (QuickTime, 14.34 MB). [URL: http://dx.doi.org/10.1117/1.2937236.2].

Using the luminescence microscope (LV200, Luminoview, Olympus Corporation, Japan), together with coelenterazine h, should therefore deliver even higher sensitivity for EMCCD detection of Ca^{2+} signals with GFP-aequorin and further improve temporal resolution.

4 Conclusions and Perspectives

Live-cell imaging using fluorescence has a number of limitations because of phototoxicity; photobleaching and the amount of excitation light used must be balanced between the quality of the image and cell viability. Bioluminescence imaging does not require light excitation, but presents the difficulty of detecting sufficient luminescence so that an image can be formed. Previous studies demonstrating the improved light emission properties of the BRET based-approach helped

resulted immediately in heterogeneous Ca^{2+} transients, detected in nearly all cells [Fig. 5(a) and Video 2]. In this representative example, compared to nonstimulated conditions, ATP stimulated large increases in the light intensity of individual cells [e.g., Fig. 5(b)]. Depending on the concentration of ATP used, many cells displayed single isolated $[Ca^{2+}]_i$ transients of short duration [5 to 10 s; Figs. 5(b) and 5(d)]. Further analysis of longer duration recordings revealed that some of these transients comprised Ca^{2+} oscillations [Fig. 5(c)].

Our studies and those of others suggest that the BRET reaction of GFP-aequorin produces a significant enhancement in the overall light output of aequorin alone.[19–21,23–25,31] The amount of light emission produced by bioluminescent reactions can be further enhanced by increasing the level of reporter expression (e.g., by viral mediated gene transfer) or by using substrates with modified light emission properties. Synthetic analogs of coelenterazine are commercially available that confer different Ca^{2+} affinities and spectral properties on aequorin,[32] and can be used instead of native coelenterazine for lower or higher sensitivity. HEK-293 cells endogenously express low levels of P2Y receptors and induce low amplitude Ca^{2+} responses,[33] and we therefore loaded cells with the ultrasensitive analog, coelenterazine h. Coelenterazine h is estimated to have a relative luminescence intensity at least ten times higher than aequorin reconstituted with native coelenterazine.[32] In this condition, high concentrations (3 mM) [Fig. 6(a) and Video 3] or low concentrations of ATP (30 μM) [Fig. 6(b) and Video 4] induced Ca^{2+} oscillations that could be readily detected using an EMCCD camera (iXon DV887, Andor Technology) attached to the baseport of a conventional microscope (Axiovert 200M, Zeiss, Germany).

Video 4 Video showing $[Ca^{2+}]_i$ rises in HEK-293 cells in response to the application of ATP (30 μM). Video corresponds to data presented in Fig. 6(b). Bioluminescent frames were each integrated for 1 s and are coded in grayscale (mean intensity/pixel range was 241 to 687) (7 frames/s). Resolution is 256×256, binning 2 (QuickTime, 6 MB). [URL: http://dx.doi.org/10.1117/1.2937236.4].

to make possible single-cell Ca^{2+} measurements using an intensified CCD (ICCD),[20] or IPD-based technologies.[21] We reproduce this approach and compare IPD performance with EMCCD. Image detection by EMCCD is facile compared with intensified devices, and allows us to easily detect receptor-driven Ca^{2+} oscillations in single cells. In as much as these are functional Ca^{2+} fluctuations representing changes between 50 and 200 nM (estimated from fura-2 measurements in cell suspensions),[33] this suggests EMCCD detection is much more sensitive than ICCD where comparable integration times are only sufficient to detect immense, nonphysiological calcium fluxes driven by application of A21387 ionophore drug in the presence of high levels (5 mM) of extracellular calcium.[20] ICCDs or cameras, such as the Electron Bombardment CCD, can also have other drawbacks such as resolution artifacts, higher noise, and lower QEs.[29] EM-CCD performance is also more comparable to IPD methods that are mostly the only recourse for single-cell Ca^{2+} detection by bioluminescence. Overall, improvements in the sensitivity provided by the Ca^{2+} sensitive probe, GFP-aequorin, and camera technologies, like the EMCCD, will extend current applications with this approach and promises to deliver high sensitivity and readout speeds for other dynamic reporter systems based on BRET.

References

1. P. A. Negulescu, N. Shastri, and M. D. Cahalan, "Intracellular calcium dependence of gene expression in single T lymphocytes," *Proc. Natl. Acad. Sci. U.S.A.* **91**(7), 2873–2877 (1994).

2. R. E. Dolmetsch, K. Xu, and R. S. Lewis, "Calcium oscillations increase the efficiency and specificity of gene expression," *Nature (London)* **392**(6679), 933–936 (1998).

3. N. R. Campbell, S. P. Podugu, and M. B. Ferrari, "Spatiotemporal characterization of short versus long duration calcium transients in embryonic muscle and their role in myofibrillogenesis," *Dev. Biol.* **292**(1), 253–264 (2006).

4. S. Schuster, M. Marhl, and T. Hofer, "Modelling of simple and complex calcium oscillations. From single-cell responses to intercellular signalling," *Eur. J. Biochem.* **269**(5), 1333–1355 (2002).

5. S. L. Shorte, W. J. Faught, and L. S. Frawley, "Spontaneous calcium oscillatory patterns in mammotropes display non-random dynamics," *Cell Calcium* **28**(3), 171–179 (2000).

6. M. Chalfie, Y. Tu, G. Euskirchen, W. W. Ward, and D. C. Prasher, "Green fluorescent protein as a marker for gene expression," *Science* **263**(5148), 802–805 (1994).

7. O. Shimomura, F. H. Johnson, and Y. Saiga, "Extraction, purification and properties of aequorin a bioluminescent protein from the luminous hydromedusan, Aequorea," *J. Cell. Comp. Physiol.* **59** 223–239 (1962).

8. O. Shimomura and F. H. Johnson, "Calcium binding, quantum yield, and emitting molecule in aequorin bioluminescence," *Nature (London)* **227**(5265), 1356–1357 (1970).

9. D. Prasher, R. O. McCann, and M. J. Cormier, "Cloning and expression of the cDNA coding for aequorin, a bioluminescent calcium-binding protein," *Biochem. Biophys. Res. Commun.* **126**(3), 1259–1268 (1985).

10. H. Morise, O. Shimomura, F. H. Johnson, and J. Winant, "Intermolecular energy transfer in the bioluminescent system of Aequorea," *Biochem.* **13**(12), 2656–2662 (1974).

11. R. Llinas, M. Sugimori, and R. B. Silver, "Microdomains of high calcium concentration in a presynaptic terminal," *Science* **256**(5057), 677–679 (1992).

12. R. Rizzuto, A. W. Simpson, M. Brini, and T. Pozzan, "Rapid changes of mitochondrial Ca2+ revealed by specifically targeted recombinant aequorin," *Nature (London)* **358**(6384), 325–327 (1992).

13. J. M. Kendall, M. N. Badminton, R. L. Dormer, and A. K. Campbell, "Changes in free calcium in the endoplasmic reticulum of living cells detected using targeted aequorin," *Anal. Biochem.* **221**(1), 173–181 (1994).

14. G. Grynkiewcz, M. Poenie, and R. Y. Tsien, "A new generation of Ca2+ indicators with greatly improved fluorescence properties," *J. Biol. Chem.* **260**(6), 3440–3450 (1985).

15. A. Miyawaki, O. Griesbeck, R. Heim, and R. Y. Tsien, "Dynamic andquantitative Ca2+ measurements using improved cameleons," *Proc. Natl. Acad. Sci. U.S.A.* **96**(5), 2135–2140 (1999).

16. T. Nagai, S. Yamada, T. Tominaga, M. Ichikawa, and A. Miyawaki, "Expanded dynamic range of fluorescent indicators for Ca(2+) by circularly permuted yellow fluorescent proteins," *Proc. Natl. Acad. Sci. U.S.A.* **101**(29), 10554–10559 (2004).

17. J. Nakai, M. Ohkura, and K. Imoto, "A high signal-to-noise Ca(2+) probe composed of a single green fluorescent protein," *Nat. Biotechnol.* **19**(2), 137–141 (2001).

18. Y. N. Tallini, M. Ohkura, B. R. Choi, G. Ji, K. Imoto, R. Doran, J. Lee, P. Plan, J. Wilson, H. B. Xin, A. Sanbe, J. Gulick, J. Mathai, J. Robbins, G. Salama, J. Nakai, and M. I. Kotlikoff, "Imaging cellular signals in the heart *in vivo*: cardiac expression of the high-signal Ca2+ indicator GCaMP2," *Proc. Natl. Acad. Sci. U.S.A.* **103**(12), 4753–4758 (2006).

19. J. R. Martin, K. L. Rogers, C. Chagneau, and P. Brulet, "*In vivo* bioluminescence imaging of Ca signalling in the brain of Drosophila," *PLoS ONE* **2**, e275 (2007).

20. V. Baubet, H. Le Mouellic, A. K. Campbell, E. Lucas-Meunier, P. Fossier, and P. Brulet, "Chimeric green fluorescent protein-aequorin as bioluminescent Ca2+ reporters at the single-cell level," *Proc. Natl. Acad. Sci. U.S.A.* **97**(13), 7260–7265 (2000).

21. K. L. Rogers, J. Stinnakre, C. Agulhon, D. Jublot, S. L. Shorte, E. J. Kremer, and P. Brulet, "Visualization of local Ca2+ dynamics with genetically encoded bioluminescent reporters," *Eur. J. Neurosci.* **21**(3), 597–610 (2005).

22. A. L. Miller, E. Karplus, and L. F. Jaffe, "Imaging [Ca2+]i with aequorin using a photon imaging detector," *Methods Cell Biol.* **40**, 305–338 (1994).

23. T. Curie, K. L. Rogers, C. Colasante, and P. Brulet, "Red-shifted aequorin-based bioluminescent reporters for *in vivo* imaging of ca(2+) signaling," *Mol. Imaging* **6**(1), 30–42 (2007).

24. K. L. Rogers, S. Picaud, E. Roncali, R. Boisgard, C. Colasante, J. Stinnakre, B. Tavitian, and P. Brulet, "Non-invasive *in vivo* imaging of calcium signaling in mice," *PLoS ONE* **2**(10), e974 (2007).

25. I. M. Manjarres, P. Chamero, B. Domingo, F. Molina, J. Llopis, M. T. Alonso, and J. Garcia-Sancho, "Red and green aequorins for simultaneousmonitoring of Ca(2+) signals from two different organelles," *Pfluegers Arch. Gesamte Physiol. Menschen Tiere* **455**(5), 961–970 (2008).

26. M. M. Knight, S. R. Roberts, D. A. Lee, and D. L. Bader, "Live cellimaging using confocal microscopy induces intracellular calcium transientsand cell death," *Am. J. Physiol.: Cell Physiol.* **284**(4), C1083–1089 (2003).

27. A. Saez-Cirion, M. A. Nicola, G. Pancino, and S. L. Shorte, "Quantitative real-time analysis of HIV-1 gene expression dynamics in single living primary cells," *Biotechnol. J.* **1**(6), 682–689 (2006).

28. J. W. Heemskerk, A. H. Westra, P. M. Linotte, K. M. Ligtvoet, W. Zbijewski, and F. J. Beekman, "Front-illuminated versus back-illuminated photon-counting CCD-based gamma camera: important consequences for spatial resolution and energy resolution," *Phys. Med. Biol.* **52**(8), N149–162 (2007).

29. C. G. Coates, D. J. Denvir, N. G. McHale, K. D. Thornbury, and M. A. Hollywood, "Optimizing low-light microscopy with back-illuminated electron multiplying charge-coupled device: enhanced sensitivity speed and resolution," *J. Biomed. Opt.* **9**(6), 1244–1252 (2004).

30. E. Karplus, "*Advances in instrumentation for detecting low-level bi-*

oluminescence in photoprotiens in bioanalysis," S. Daunert and S. Deo, Eds., Wiley-VCH, pp. 199–223 (2005).

31. A. Niedernberg, S. Tunaru, A. Blaukat, A. Ardati, and E. Kostenis, "Sphingosine 1-phosphate and dioleoylphosphatidic acid are low affinity agonists for the orphan receptor GPR63," *Cell Signal* **15**(4), 435–446 (2003).

32. O. Shimomura, B. Musicki, and Y. Kishi, "Semi-synthetic aequorins with improved sensitivity to Ca2+ ions," *Biochem. J.* **261**(3), 913–920 (1989).

33. E. Adinolfi, M. G. Callegari, D. Ferrari, C. Bolognesi, M. Minelli, M. R. Wieckowski, P. Pinton, R. Rizzuto, and F. Di Virgilio, "Basal activation of the P2X7 ATP receptor elevates mitochondrial calcium and potential increases cellular ATP levels, and promotes serum-independent growth," *Mol. Biol. Cell* **16**(7), 3260–3272 (2005).